Nuclear Engineering and Technology 49 (2017) 1250–1258

Contents lists available at ScienceDirect

Nuclear Engineering and Technology

journal homepage: www.elsevier.com/locate/net

Original Article

SIMMER extension for multigroup energy structure search using genetic algorithm with different fitness functions

Mattia Massone*, Fabrizio Gabrielli, Andrei Rineiski

Karlsruhe Institute of Technology (KIT), Hermann-von-Helmholtz-Platz 1, Eggenstein-Leopoldshafen, D-76344, Germany

ARTICLE INFO

Article history:
Received 23 May 2017
Received in revised form
24 July 2017
Accepted 26 July 2017
Available online 2 August 2017

Keywords:
Multigroup cross section
Energy grouping
Genetic algorithm
Reactor safety
Fitness function
M&C2017

ABSTRACT

The multigroup transport theory is the basis for many neutronics modules. A significant point of the cross-section (XS) generation procedure is the choice of the energy groups' boundaries in the XS libraries, which must be carefully selected as an unsuitable energy meshing can easily lead to inaccurate results. This decision can require considerable effort and is particularly difficult for the common user, especially if not well-versed in reactor physics. This work investigates a genetic algorithm-based tool which selects an appropriate XS energy structure (ES) specific for the considered problem, to be used for the condensation of a fine multigroup library. The procedure is accelerated by results storage and fitness calculation speed-up and can be easily parallelized. The extension is applied to the coupled code SIMMER and tested on the European Sustainable Nuclear Industrial Initiative (ESNII+) Advanced Sodium Technological Reactor for Industrial Demonstration (ASTRID)-like reactor system with different fitness functions. The results show that, when the libraries are condensed based on the ESs suggested by the algorithm, the code actually returns the correct multiplication factor, in both reference and voided conditions. The computational effort reduction obtained by using the condensed library rather than the fine one is assessed and is much higher than the time required for the ES search.

1. Introduction

SIMMER [1,2] is a multi-velocity-field, multiphase, multicomponent, Eulerian fluid-dynamics code coupled with a space-dependent neutron transport kinetics model, primarily developed for safety studies on liquid-metal-cooled fast reactors. During the simulation, the neutronics module of SIMMER employs macroscopic cross-sections (XSs) with a broad-groups energy structure (ES) as input libraries, which are originally obtained from the pointwise libraries or by collapsing the reference libraries at several hundreds of energy groups available at the Karlsruhe Institute of Technology (KIT) with a weighting function (neutron spectrum) specified by the user.

A code extension that allows including the collapsing procedure inside SIMMER has already been proposed [3]. In this way, the energy discretization of the XSs actually used in the transport calculation, referred to as broad-groups libraries (BL), can be coarser than that of the input libraries, hence denoted fine-libraries (FL). The XSs obtained from these libraries are collapsed at each time step with the advantage that the collapsing is done with neutron spectra obtained for the transient conditions in each core subregion.

A particular difficulty for the user is the choice of the optimal broad-group ES to be used, which might have a significant impact on the results [3]. Since no automatic tools are available to fulfill this goal, the choice of the optimal broad-group ES is left to the user, who must have good knowledge of neutronics and has often to perform investigations of the different options to avoid nonoptimal or misleading solutions.

Having this in mind, the employment of an evolutionary genetic algorithm (GA) in the SIMMER environment has been proposed in the past [4,5] to compute the most “proper” broad energy group discretization for transient analyses. Similar approaches, focused on swarm algorithms, have been followed in the past by Yi and Sjoden [6] and Mosca et al. [7,8] for both single pins in thermal reactors and infinite homogeneous problems in fast systems. An open point is the fitness function (FF) to be used in the GA: the multiplication factor, used in [4–7], is an integral value, and could hence be affected by compensation effects.

The computational expense required by the GA is fully compensated by its advantage: by using the optimal ES for the XS collapsing, it is possible to perform neutronics calculations having

* Corresponding author.
E-mail address: mattia.massone@kit.edu (M. Massone).

http://dx.doi.org/10.1016/j.net.2017.07.012

nearly the same accuracy as using the FL and the computational time of the BL. This advantage proves particularly important if the transport calculation must be repeated for a large number of times, as in the case of transient computations with SIMMER. Moreover, since the optimal ES is not expected to change significantly if the system geometry is not deeply altered, the GA must not be performed for each simulation of the same system. This work expands the work on the SIMMER extension presented in [4] and [5], investigating the effect of different FF on the results. The best found ESs are applied also in the case of voided conditions, showing that the discrepancies in the multiplication factor are small. Finally the computational expense is assessed and compared with the time reduction owing to using the BL rather than the FL.

2. Description of the actual work

GAs [9–11] are a widely used type of metaheuristics for search and optimization, based on the principles of Darwinian selection and evolution (on which the wider set of evolutionary algorithms is founded).

The starting point of a GA is a collection (using the analogy of biology, denoted by population) of possible solutions (individuals), characterized by a set of properties (genes), usually randomly generated; the members of the population are tested and used to produce a new population (next generation), based on a measure of their adequateness as a problem solution called "fitness". As the iterations (Fig. 1) go on, the solution space is explored and the quality of the population grows, eventually approaching the optimal (or at least a reasonably reliable) solution, similarly to natural evolution [11].

2.1. Chromosome representation

The way of representing the individual genes set (chromosome) is highly problem-specific and is the first point to be addressed when setting a GA up.

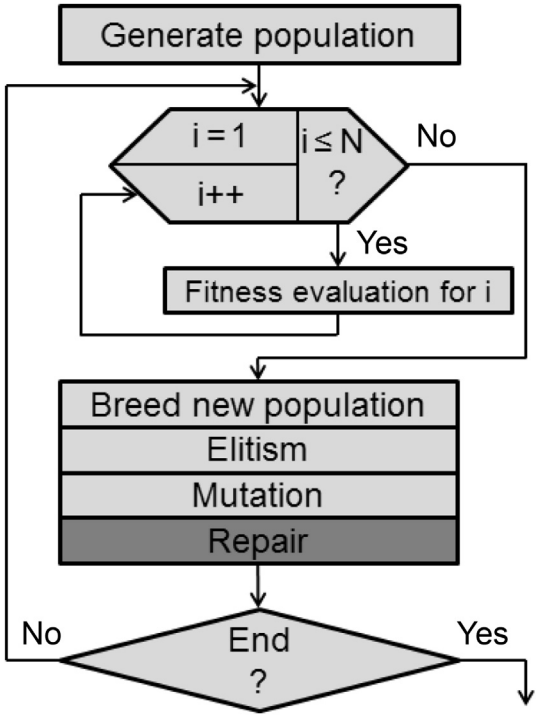

Fig. 1. Genetic algorithm (GA) flowchart [5]. Repair block is specific for the current application due to the chosen chromosome representation. i denotes the i-th individual of the N-sized population.

The specific constraints applicable to this case are two:

I. The gene pool is finite, i.e., the energy cuts of the BL can be set only just at the ones present in the FL.
II. The number of energy cuts to be set, i.e., the number of energy groups of the BL, is fixed *ab initio*.

A nonbinary representation (Fig. 2) has been chosen, consisting of chromosomes with a number of genes *FG*-1; each gene can assume any integer value (allele) of the interval (1,*MG*], representing the first fine-group belonging to a broad energy group. It is implicit that the original and the collapsed libraries share the same starting energy. Constraint II can be enforced by making sure that each allele does not appear twice in the chromosome.

Sorting of the genes based on their alleles has pros and cons; experience suggests that sorted chromosomes give better results [4].

2.2. Fitness function

As for any evolutionary algorithm, an FF is required to rank the solutions based on their suitability in solving the problem. This function represents in biological systems the reproductive success, at the base of natural selection and evolution.

Different options are possible, but the required computational expense should be taken into account, as the FF must be evaluated for each individual of each generation.

Similarly to Yi and Sjoden [6], a simple and suitable FF is considered to be:

$$f_I^{(k)} = \left| k_{\text{eff}}^{I} - k_{\text{eff}}^{\text{obj}} \right| \cdot 10^5, \tag{1}$$

where the objective k_{eff} can be easily identified performing an eigenvalue calculation with the original uncollapsed FL.

The multiplication factor, however, is an integral parameter, condensing in a single value many different pieces of information and probably hiding compensation effects. A more adequate measure of the ES effectiveness can be considered the match of the flux spectrum before and after the collapsing. Assuming that a perfect XS collapsing would make:

$$\Phi_G^{\text{BL}} = \Phi_G^{(\text{FL})} \doteq \sum_{g=C(G-1)}^{C(G)-1} \Phi_g^{(\text{FL})}, \tag{2}$$

the spectrum difference in a single mesh cell can be evaluated as:

$$\Xi = \cos\xi = \frac{\sum_{G=1}^{MG} \left[\Phi_G^{(\text{BL})} \cdot \Phi_G^{(\text{FL})} \right]}{\left\| \Phi^{(\text{BL})} \right\| \cdot \left\| \Phi^{(\text{FL})} \right\|}, \tag{3}$$

which is the cosine of the angle between the two flux vectors in phase space with FG dimensions (Fig. 3). This parameter is closely connected with the Pearson correlation coefficient [12].

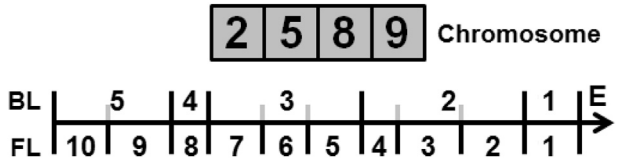

Fig. 2. Example of 5-groups broad-groups libraries (BL) collapsed from 10-groups fine-libraries (FL) based on the chromosome (2, 5, 8, 9).

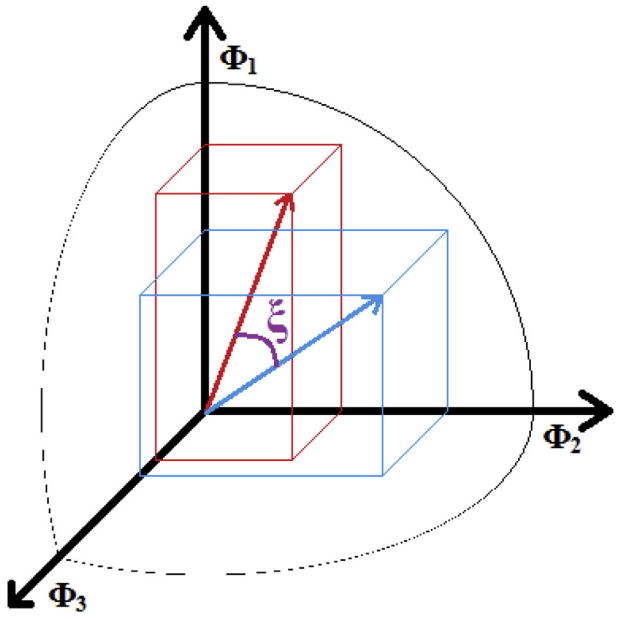

Fig. 3. Multigroup neutron flux phase space with 3 groups.

However, in order to condense the information of all system cells into a single value, the FF is defined as:

$$f_I^{(\Phi)} = \frac{1}{\pi}\arccos\frac{\sum_{i=1}^{N_{\text{cells}}} \Xi_i}{N_{\text{cells}}}, \tag{4}$$

whose value is bounded between 0 and 0.5 (each component of the neutron flux is positive, due to physical reasons).

A combination of the two FFs is also possible. However, as the two components have different metrics, the geometric average must be used to give the same importance to both components:

$$f_I^{\text{comb}} = \sqrt{f_I^{(k)} \cdot f_I^{(\Phi)}}. \tag{5}$$

2.3. Computational expense reduction

As the alleles are chosen from a discrete set, there is quite a chance of examining the same individual twice. The probability of this occurring is actually much higher than predicted by simple combination counting, as each generation depends on the previous one. Repeating the evaluation of the fitness, of course, must be avoided to the utmost, as it is the most expensive operation of the GA. Hence a left-child right-sibling binary tree [13] storage is implemented (Fig. 4), keeping track of all explored configurations and of their fitness; the tree is searched for each individual before performing the eigenvalue calculation, which can be skipped if the

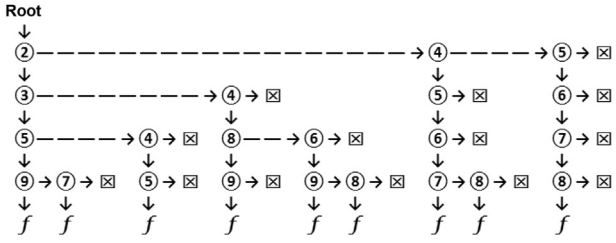

Fig. 4. Storage tree example for 9 to 5 groups collapsing.

required fitness is already known. For searching a given chromosome, the 1st gene is compared with the root node: in case their values match, the search continues comparing the next gene with the left child of the previous node; whenever there is a discrepancy between the gene and the node, instead, the gene is tested with the right child of the node. In case all genes have been successfully found, the final node of the followed branch (the leaf) contains the required fitness. On the contrary, finding a leaf after following a right branch means that the searched chromosome has never been examined before, and the fitness must be calculated; at this point, however, the new individual can be stored with its fitness in a new branch of the tree, starting from the position of the encountered right leaf. The chosen storage structure combines simplicity, rapidity in the search, and reduced space (which is allocated, as in a linked list, only when it is needed) requirements. The time spent in creating, keeping, and deallocating the tree is amply compensated by the spared calculations.

Also, fitness estimation itself is accelerated: the eigenvalue calculation with the FL produces, along with the objective k_{eff}, the neutron fluxes with the uncollapsed ES. If these fluxes are collapsed (following each individual chromosome), with the formula:

$$\phi_G = \sum_{g=C(G-1)}^{C(G)-1} \phi_g, \tag{6}$$

they represent a well educated guess for the transport solver, which then is able to converge to the solution of the eigenvalue calculation within a few iterations.

Finally, as each individual of a generation is completely independent from the others, the algorithm is very suitable for an efficient parallelization.

2.4. Genetic operators

As selection operator, the tournament method [14] is chosen, mainly for being easily tunable. The individuals selected with this method constitute the mating pool, from which couples (Fig. 5) are randomly extracted to create two offspring through one-point crossover (XO). When the reproduction phase is finished, the parents are all discarded (nonoverlapping population model), with the exception of the best-performing ones, which are passed to the next generation unchanged (elitism).

Genetic diversity is improved by mutation: once the next generation is established, a fixed number of randomly chosen genes have their value replaced with another randomly chosen allele. This procedure improves the diversity of the genetic pool, may reintroduce extinct alleles, and opposes to genetic drift.

2.4.1. Chromosome repair

The chosen representation stipulates that each allele appears in a chromosome at most once; nevertheless, after mutation or

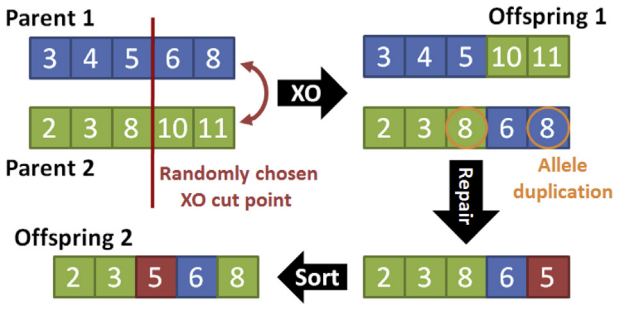

Fig. 5. Example of one-point crossover (XO) and repair.

crossover, such duplications can occur. Hence, one requires a chromosome repair mechanism, which must not be too invasive, in order to avoid excessive perturbation of the natural selection process.

Therefore, after the new generation has been created, all individuals are checked for duplication errors. If such errors are observed, a mutation of the genes with duplicated alleles is performed (Fig. 5) until all damaged chromosomes are fixed.

2.5. Test configuration

The aim of the test procedure is finding an ES with 11 energy groups starting from the 72-groups XS data libraries (Table 1) developed at KIT for SIMMER analyses [15] able to reproduce the reference results with respect to the criticality level and the Doppler and coolant reactivity feedbacks in a fast reactor system. The number of groups of the final ES, which can be defined by the user, has been chosen as most of the mechanistic calculations with SIMMER at KIT are performed using an 11-groups library [16]. Such a number of groups is deemed a good compromise between computational time reduction (see §3.2) and effective representation of the energy spectrum in different conditions. In fact, one expects that the smaller the number of groups, the more the optimal solution found by the GA is tailored to the test system conditions. In other words, the "neighborhood of the system conditions" for which the optimal ES is still valid becomes smaller as the number of groups used is reduced, i.e., the applicability of the ES in a transient (or for the calculation of feedback coefficients) is lowered.

2.5.1. Algorithm configuration

While for most applications a suboptimal solution is probably sufficient to achieve good results, in this case the algorithm is configured with very tight parameters in order to achieve refined results, more suitable for the study of the position of the energy cuts.

Each generation is composed of 500 individuals, a large number intentionally chosen to allow a large number of copies of each allele and so limit the genetic drift effect.

Table 1
Upper energy boundaries of the broad-groups libraries (BL) [15].

Group	BL groups	Group	BL groups	Group	BL groups
1	2.000E+07[a]	25	1.228E+05	49	3.355E+03
2	6.703E+06	26	1.111E+05	50	2.747E+03
3	3.679E+06	27	9.482E+04	51	2.249E+03
4	3.012E+06	28	8.230E+04	52	2.035E+03
5	2.466E+06	29	6.738E+04	53	1.722E+03
6	2.019E+06	30	5.517E+04	54	1.507E+03
7	1.653E+06	31	4.748E+04	55	1.434E+03
8	1.353E+06	32	4.087E+04	56	1.234E+03
9	1.108E+06[a]	33	3.698E+04	57	1.010E+03
10	9.072E+05	34	2.928E+04	58	7.485E+02
11	8.209E+05[a]	35	2.739E+04	59	5.545E+02[a]
12	7.065E+05	36	2.479E+04	60	4.540E+02
13	6.081E+05	37	2.029E+04	61	3.043E+02
14	5.502E+05	38	1.662E+04	62	2.040E+02
15	4.979E+05	39	1.503E+04	63	1.367E+02
16	4.505E+05	40	1.273E+04	64	9.166E+01[a]
17	4.076E+05	41	1.114E+04	65	4.552E+01
18	3.508E+05	42	9.119E+03	66	1.945E+01
19	3.020E+05	43	7.466E+03	67	9.906E+00[a]
20	2.732E+05[a]	44	6.320E+03	68	5.043E+00
21	2.472E+05[a]	45	5.531E+03	69	2.130E+00
22	2.128E+05[a]	46	5.005E+03	70	1.020E+00
23	1.832E+05	47	4.166E+03	71	4.850E−01[a]
24	1.500E+05[a]	48	3.527E+03	72	1.890E−01

[a] Best estimated energy structure (ES) groups for the reference configurations.

The selection pressure is kept to a low level by using 100 tournaments without replacement (all individuals of the population participate in exactly 1 tournament) of the stochastic type, i.e., all participants of the tournament are included in the mating pool with a number of copies:

$$M_I = (1-p)^{R_I - 1} \tag{7}$$

with $p = 0.1$.

Finally, 5% of the chromosomes of the next generation are mutated and the top 2% of each generation passes to the next one with the elitist mechanism.

In order to reduce the stochastic effect in the results, the GA is carried out five times with each FF; in each run, 50 generations are examined. The calculation has also been repeated two times more with the core in voided conditions, in order to study the effects on the energy discretization on the feedback effect.

2.5.2. Test system description

The test system is the Advanced Sodium Technological Reactor for Industrial Demonstration (ASTRID) (17) at End of Cycle, studied at KIT in the framework of the European Sustainable Nuclear Industrial Initiative (ESNII+).

The considered ASTRID core is a 1500 MW_{th} with two fuel zones (Fig. 6), including 177 and 114 fuel subassemblies, with different enrichment of the (U, Pu)O_2 fuel. The core voided configuration is obtained removing the sodium coolant from all the fuel zones and from the intermediate fertile zone, the coolant in the inter-SA gaps being not removed.

3. Results

The results show that the employment of the GA in the SIMMER framework does make the code able to find a broad ES which can reproduce the reference structure. It is interesting to analyze the results shown in Figs. 7–10 and investigate the physical reasons that guide the evolution.

From Fig. 7, it is clear that a pattern associated with good results in terms of fitness coefficient exists. The figure is particularly effective in showing the groups that should not be separated, namely the ones between ~30 keV and 500 eV; this energy range, as shown in Fig. 10, corresponds with the largest resonance of sodium and with most of the U^{238} large resonances.

Fig. 8 shows that an energy cut at Group 9 (~1.1 MeV, see Table 1) occurs in more than 50% of the best solutions, regardless of the FF used; however, if the k_{eff} FF is used, the position can be shifted to

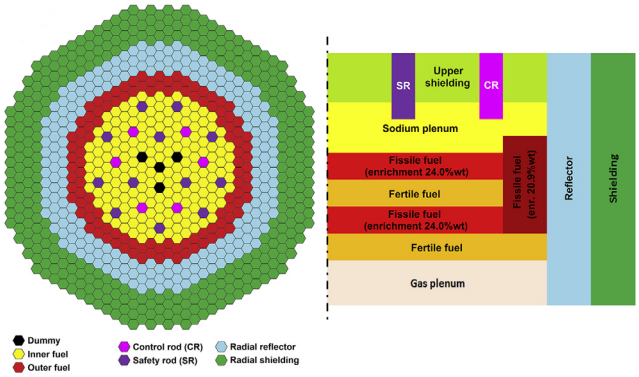

Fig. 6. Advanced sodium technological reactor for industrial demonstration (ASTRID)-like core map and vertical section at end of cycle (EOC), based on [17].

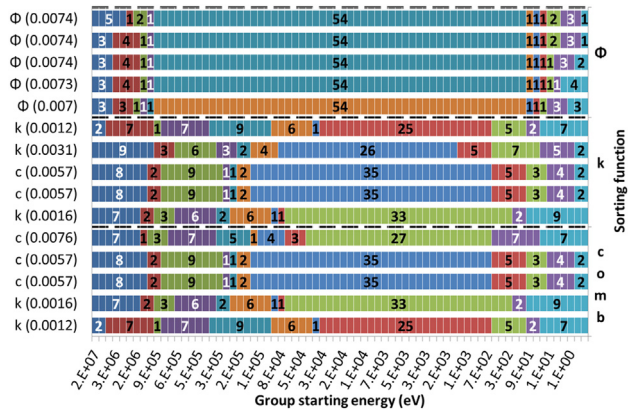

Fig. 7. Best found energy structures (ESs), rated based on the different fitness function (FF), associated with used FF and corresponding fitness (expressed in term of the sorting function). k, Φ and comb denote the FF used, respectively $f^{(k)}$, $f^{(\Phi)}$ and $f^{(comb)}$.

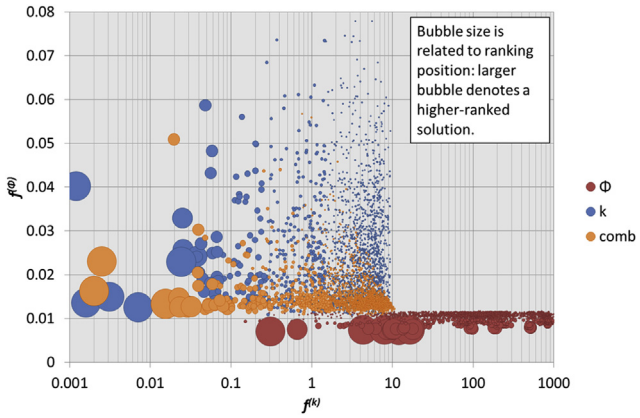

Fig. 9. Performance of the best 500 solutions found in each genetic algorithm (GA) run, based on multiplication factor FF [$f^{(k)}$] and flux-based FF [$f^{(\Phi)}$], sorted based on the fitness function (FF) used for the calculation.

Group 10 or Group 11. One can consider this cut as the limit between resonance and fast region [4].

Fig. 8 also displays the need for some detail in the discretization of the low energy zone: the need for energy cuts at Group 59 and Group 64 is particularly clear with both k_{eff} FF and combined FF. This effect, that might be unexpected in a fast reactor, can be explained by the presence of important resonances in the energy region (Fig. 10), which cannot be ignored in the condensation process.

One immediately notices in Fig. 7 how much the FF choice influences the results. When flux-based FF [$f^{(\Phi)}$] is used, the best solutions present an extremely large group in the central zone of the energy space, with 10 very small groups at the two sides, the distribution of which plays a small role on the fitness. Fig. 8 confirms that the central group should be very wide to minimize the FF, even if the boundaries position is less defined than in Fig. 7. Of course, such an ES cannot adequately describe the energy space, as 900 keV neutrons cannot be distinguished from 90 eV ones. These results represent a side effect of the way the GA tackles the problem; while looking for the best ES, the algorithm has found a "shortcut": by making one component of the flux vector dominant over the other ones, i.e., by creating a single massive group and several small ones, both the objective and the calculated vector will lie on the component hyperspace axis, and so assume the same direction. This does not mean that this FF cannot find really useful results, but one should temper the risk of the system being misled by trivial solutions.

The combination of the flux criterion with the fitness one effectively does so. Fig. 9 shows how the combined FF can limit the occurrence of solutions with too high discrepancies, in both directions. One can also notice that multiplication factor FF [$f^{(k)}$] is able to obtain an ES with comparable performance to those obtained with combined FF [$f^{(comb)}$], also in terms of flux direction; this is clear also from Fig. 7, where the best ESs in terms of k_{eff} are also included among those sorted with the combined FF, and vice versa. This suggests that a relation between good k_{eff} estimate and good flux representation exists; the inverse relation, instead, for the reason discussed in the previous paragraph, cannot hold.

Based on previous results, one can consider $f^{(comb)}$ as a better compromise on the FF than $f^{(k)}$, and so the best ES obtained with this method, will be considered the best ES found.

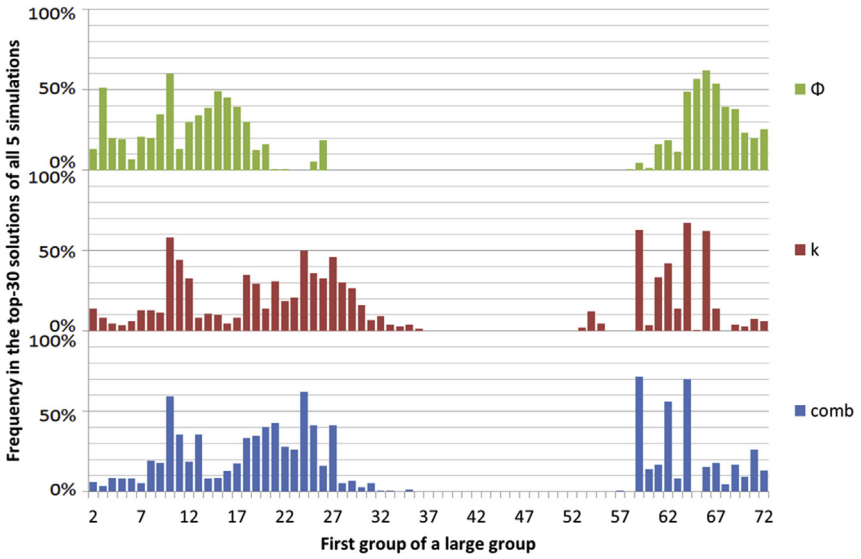

Fig. 8. Frequency of groups as broad-groups libraries (BL) groups starters in the top 30 solutions of each of the five simulations, divided based on the fitness function (FF) used.

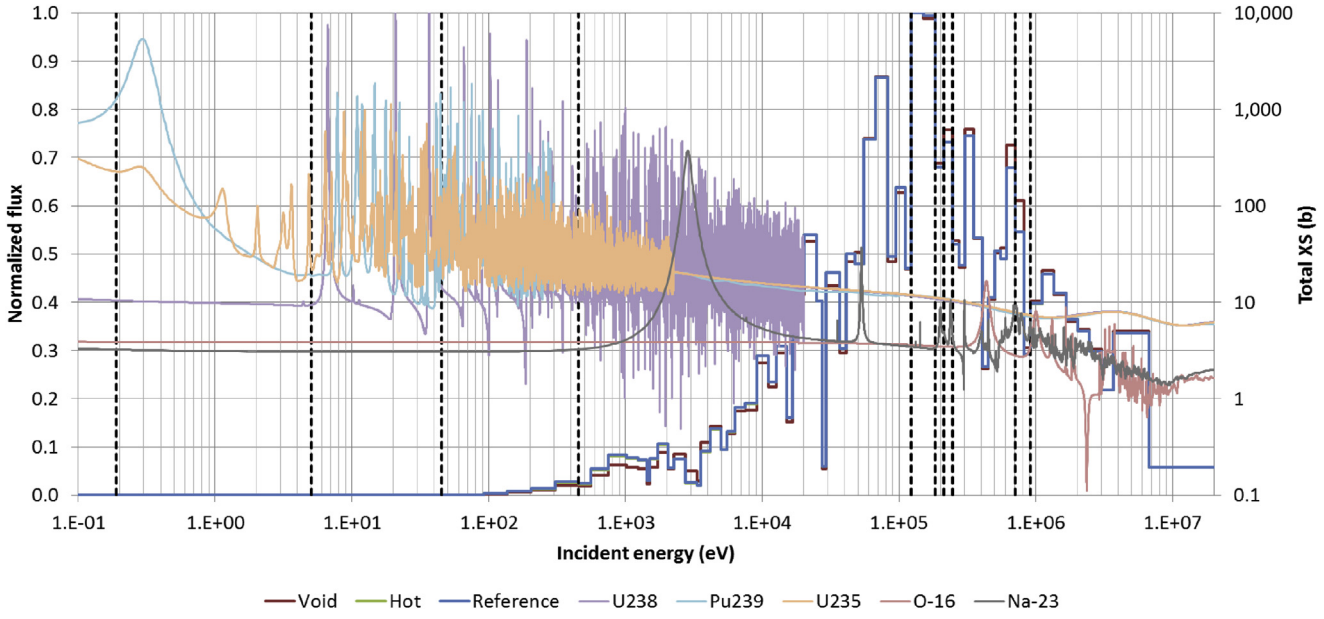

Fig. 10. Advanced sodium technological reactor for industrial demonstration (ASTRID) neutron spectrum in a fuel cell (in reference and voided conditions), relevant nuclides total cross-sections (XSs), and best energy structure (ES) found using combined FF [$f^{comb)}$].

3.1. Feedback coefficients

The feedback coefficients are key parameters for the reactor design; hence, it is very important that the new ESs provide correct estimates of the k_{eff} also in conditions which are not those used for the GA run, so that the transient results are reliable at least until core degradation starts. For analyzing the next accidental phases, characterized by full core degradation, a new run of the GA may be necessary.

In order to verify this, the reference coefficients (i.e., calculated with all 72 available groups) are compared with the ones obtained using the GA best solution. As further proof, the GA has been applied to the voided core, and the corresponding best solution has also been used to calculate the feedback coefficients. Table 2 summarizes the results.

Both reference and voided condition solutions provide excellent results for both coolant void and Doppler feedback coefficients, with errors on the k_{eff} in the order of 20–30 pcm. The important values, i.e., the feedback coefficients, present even lower errors, acceptable for most applications.

This means that the reference conditions ES are not expected to lead to incorrect results in accidental conditions. However, the presence of compensation among different energy groups cannot be excluded.

Table 3 and Fig. 11 show the effectiveness of the different FFs in obtaining ES predicting the correct feedback coefficient. With both the multiplication coefficient FF (Eq. 1) and the combined FF (Eq. 6), the GA returns in all five calculation runs an ES that predicts the feedback coefficients with a discrepancy lower than 40 pcm (30 pcm for the void feedback coefficient), a value compatible with most uses. This means that using the GA combined with these FFs is safe, as it is unlikely that the advised ES returns an incorrect feedback coefficient, undermining the simulation reliability in accident scenario simulations.

In addition, Fig. 11 shows that the combined FF has to be preferred over the k_{eff} one, as it lowers the discrepancy on the feedback coefficients both on average and considering one standard deviation; at the same time, the multiplication factor is calculated with less than 1 pcm discrepancy.

On the contrary, the flux criterion is not reliable if not tempered by the k_{eff} one as it leads to ES that, on average, produce discrepancies almost three times larger than the combined FF ones. Also,

Table 2
Impact of energy structure (ES) on the feedback coefficients.

	Fine libraries	Best ES (reference configuration)	Best ES (void configuration)
***k*eff**			
Reference	0.99919	0.99920	0.99932
Voided core	1.00995	1.01002	1.00996
T_{fuel} +1000 K	0.99633	0.99640	0.99669
Feedback coefficients (pcm)			
Core void	+1066	+1072	+1054
K_D	−560	−548	−515

$K_{D,\ Doppler\ feedback\ coefficient}$; $T_{fuel,\ fuel\ temperature}$.

Table 3
Feedback coefficients with best energy structure (ES) of each case, depending on the used fitness function (FF). Five genetic algorithm (GA) runs per FF are shown.

k_{eff}	Core void feedback coefficient (pcm)	K_D (pcm)
***f*(*k*)**		
0.99919	+1055	−523
0.99918	+1039	−534
0.99918	+1039	−534
0.99919	+1057	−546
0.99918	+1053	−534
***f*(*comb*)**		
0.99919	+1054	−552
0.99920	+1072	−548
0.99920	+1072	−548
0.99919	+1053	−525
0.99919	+1054	−525
***f*(*Φ*)**		
0.99697	+1013	−468
0.99403	+1102	−507
0.99798	+1047	−550
0.99919	+1149	−534
0.99734	+1014	−460

$f^{(comb)}$, combined FF; $f^{(k)}$, multiplication factor FF; $f^{(\Phi)}$, flux-based FF; $K_{D,\ Doppler\ feedback\ coefficient}$.

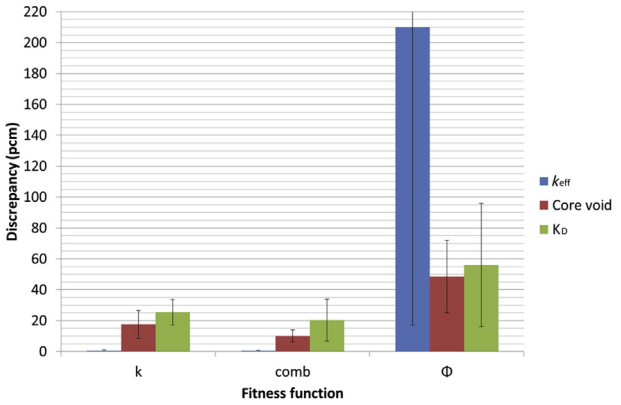

Fig. 11. Average discrepancy and standard deviation of the feedback coefficients with the solutions found by the five runs with each fitness function (FF). comb, kand Φ denote the used FF, respectively $f^{(comb)}$, $f^{(k)}$ and $f^{(\Phi)}$. K_D, Doppler feedback coefficient.

the high standard deviation shows that the results are largely variable. This means that, based on the "luck" in the GA random sampling, the calculated ES could predict a k_{eff} with a 500 pcm discrepancy (Table 3, 2nd case) or a feedback coefficient 100 pcm higher than expected (Table 3, K_D, 5th case).

3.2. Time performance

For the purpose of this study it is important to evaluate the time performances of both the GA and SIMMER with the XS collapsing. Thus, one can demonstrate that the time spent for the ES determination can be entirely covered by the corresponding reduction of the XS collapsing. The latter procedure can indeed be used without ES search, but this approach should be discouraged as results can be affected by large errors if the chosen ES is inappropriate.

The time performance measurement has been carried out using the Intel VTune Amplifier 2015 (Intel, Santa Clara, CA, USA) profiler on a node with exclusive access of the InstitutsCluster II (IC2) (Karlsruhe, BW, Germany) [18], with processor Intel Xeon 5 (2.6 GHz) (Intel, Santa Clara, CA, USA).

3.2.1. Central processing unit time required for the GA

In order to have uniform results, in each run the GA performs six generations with 50 individuals each. The measurement has been repeated four times for better results precision. Nevertheless, due to the stochastic choices intrinsic to the GA, the number of actual FF to be evaluated changes; in addition the fitness of any already examined individual is just retrieved from the storage tree, an operation which is much faster than the actual FF calculation. The FF used is based on the multiplication coefficient. The results are shown in Table 4 and averaged in Table 5.

The final adjoint and real calculation, as expected, is longer than the doubled FF evaluation time as the flux acceleration described in §2.3 is not applied.

Except for the time invested in objective k_{eff} calculation, which depends only on the FL, the other computational time values are representative only if ESs with 11 groups are searched.

3.2.2. XS collapsing time reduction

A 10 s stationary approach calculation of the ESNII+ core has been used for the estimation of the computational time of a SIMMER simulation. Both the actual central processing unit (CPU) time and the neutronics/fluid-dynamics time share, of course, strongly depend on the model (number of thermal-hydraulic cells, neutronic mesh fineness, transient type, reactor state…). In order to reduce measurement uncertainty, calculations have been repeated three times for each considered number of groups, with three different ESs, in the same conditions described in the previous paragraph.

Results in Fig. 12 show the CPU time dependence on the number of groups used: while thermal-hydraulics and XS processing time are not affected, the time required by the transport solver increases more than linearly with the number of groups. The time required by the XS collapsing procedure is almost negligible, being ~40 s in all cases, i.e., 0.4% of the total CPU time at most (72→5 groups). The XS processing time is constant, as this procedure is performed on the FL, which has 72 groups in all considered cases.

Table 4
Genetic algorithm (GA) computational time tests.

	Test 1	Test 2	Test 3	Test 4
Individuals	300	300	300	300
FF calculations	262	249	250	259
Computational time per section (s)				
Total	1982.5	1945.9	1917.6	1951.2
Objective k_{eff}	58.0	57.8	58.0	56.4
Individuals FF	1899.2	1868.4	1837.3	1880.0
Final k_{eff} and k^+	24.6	19.1	21.7	14.2
SIMMER frame	0.7	0.6	0.6	0.6

FF, fitness function; k^+, adjoint problem eigenvalue.

Table 5
Genetic algorithm (GA) average computational time results (s).

	Average	Corrected sample σ
Objective k_{eff}	57.5	0.8
FF calculation per individual	7.3	0.1
Final k_{eff} and k^+	19.9	4.4
SIMMER frame	0.6	0.03

FF, fitness function; k^+, adjoint problem eigenvalue.

3.2.3. GA convergence speed

Estimating the number of individuals to be examined before convergence to a reasonable ES is not an easy task: it requires sensitivity studies on all different GA parameters, such as initial population size, growth rate, mutation rate, and selection pressure. Such tests would allow estimating the minimum number of individuals that, on average, are needed for convergence. These optimization studies are considered of interest for the future, along with the evolution of the GA to an Adaptive Genetic Algorithm [19], which would improve the convergence rate.

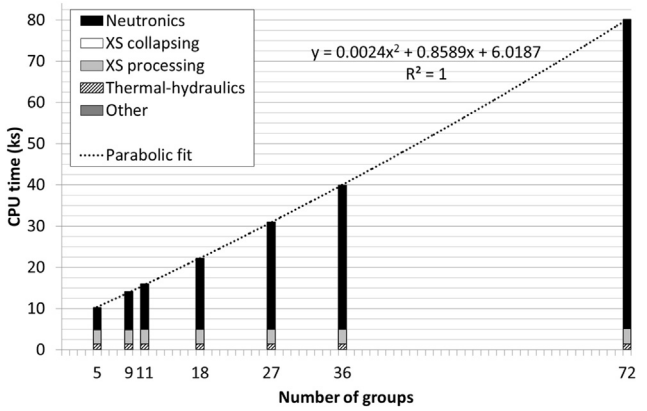

Fig. 12. Computational time for 10 s of stationary approach calculation with different number of groups using best estimated energy structures (ESs) [10]. XS, cross-section.

Table 6
Configuration and results of the genetic algorithm (GA) convergence speed tests.

Initial population	50	100	150
Growth rate	1.0	1.0	1.0
Mutation rate (%)	5	5	5
Elitism rate (%)	2	2	2
Number of tournaments	10	20	30
Tournament parameter (p)	0.1	0.1	0.1
Number of generations	16	39	20
	40	35	18
Considered individuals	800	3,900	3,000
	2,000	3,500	2,700
Unique individuals	650	3,106	2,715
	1,553	2,985	2,434

A preliminary estimate of the number of individuals required for the 72→11 groups collapsing problem has been done. The GA has been run with three different population sizes (twice each), keeping the selection pressure constant (5 individuals per tournament on average). The termination criterion is the achievement of a fitness value lower than 1, i.e., a discrepancy on the multiplication factor in the order of 1 pcm; such a difference is considered acceptable for most types of calculation.

The results summarized in Table 6 suggest that a smaller initial population converges faster to the solution; Fig. 13 shows that the convergence of such populations is more erratic, being more susceptible to initial random sampling and genetic drift. Also, a faster convergence of the population average fit might not be an advantage, as the lower genetic variability would affect the exploration capability of the population, which could end up prematurely converging toward a local optimum. The convergence speed point should be studied more in depth, considering different FF, mutation rates, and tournament parameters, but the performed calculations provide a preliminary average number of unique individuals required to achieve convergence, being for the present case 2241 ± 956.

Based on the results shown in Fig. 12, a calculation with 11 energy groups would reduce the computational time with respect to the 72 groups BL case by 64 ks (80%) for the first 10 s of simulation. Combining this result with Table 5 data, the same computational time can be used to take into consideration more than 8,500 unique solutions, more than double the required estimate increased by 2σ.

Moreover, the ES has to be calculated only once for each reactor system, but can be used for different simulations, provided that the reactor conditions do not change excessively. Finally, the CPU time reduction has been calculated for 10 s of simulations, but much longer time spans (at least a few minutes of simulation) have to be considered when performing safety studies, making the time reduction in absolute terms extremely favorable.

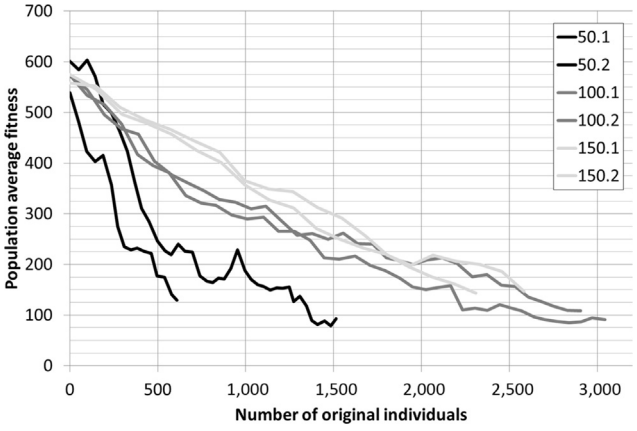

Fig. 13. Population average fitness convergence speed.

4. Conclusions

An automated tool aiming to the energy meshing selection for multigroup XS libraries has been presented. The procedure is based on a GA and is coupled with the safety analysis code SIMMER. The tests performed on the ESNII+ ASTRID-like reactor system show that the GA is able to suggest ESs for the considered problem, which correctly predict the multiplication factor both in reference and out-of-nominal conditions.

The problem constraints have been established and a non-binary chromosome representation able to respect them has been devised. The genetic operators have been chosen in order to respect the problem boundaries and to leave the user the freedom of both choosing the number of groups in the solution and easily tuning the GA parameters.

Three different FFs, i.e., the measure of the studied solution "goodness", have been examined. While good results can be obtained using an FF based only on the difference between the k_{eff} obtained with the considered ES and the objective one, the GA benefits from the combination with the cosine between the objective and the calculated flux vectors in the energy space. On the contrary, the results show that the use of the FF based on the flux alone is unsafe, as the algorithm is likely to tend toward degenerate cases, with a single energy group enclosing most of the energy spectrum.

The fitness calculations are the operations employing most of the computational time, so the procedure has been accelerated using a binary tree, where new fitness values are stored as they are calculated to be retrieved in case they are needed again, and by collapsing the flux calculated with the FL, which provides an educated guess to the transport solver and so faster convergence.

The tests focus on the search of an 11-groups ES for the collapsing of the 72-groups FL. The ES determined by the GA adequately models the reactor in reference conditions, demonstrating the effectiveness of the approach in the problem solution. The GA has also been applied to the reactor in out-of-nominal conditions; the study is of interest to predict the effect of the ES on accidental transient simulations. The results show that the discrepancies of the feedback coefficients are acceptable in all considered cases, both when the ES is calculated with the reactor in its reference state and when a voided configuration is used. The discrepancy is particularly small if the combined FF is used instead of the k_{eff}-based one; ESs obtained with the flux-based FF, instead, are often unable to provide appropriate estimate of the feedback coefficient.

The computational time in a selected 10 s transient is dominated by the transport solver, so it can be strongly reduced by using XS libraries with less energy groups; results show that the link between CPU time and number of energy groups is quadratic. Based on the parabolic fit, XS collapsing from 72 energy groups to 11 energy groups is able to reduce the CPU time by 80%. This, considering that accidental transient SIMMER calculations can take days or even weeks, makes the XS collapsing an extremely powerful tool, if one is able to use the correct ES. The GA cares for this last point.

Preliminary results suggest that on average 2,241 individuals have to be examined before the discrepancy on the multiplication factor is reduced to the order of 1 pcm, acceptable for most applications. Considering that the FF evaluation takes 7.3 s per individual, the GA would converge within just a small fraction of the spared time; moreover, one should consider that the ES can be used for all simulations related to the reactor, provided that the initial conditions do not change too much.

Finally, the convergence speed can be improved by optimization of the parameters and by passing to Adaptive Genetic Algorithm; both activities considered of interest for future studies. Also, the methodology can be improved by further investigating other FFs

options, possibly taking into account the reaction rates, which play a relevant role on the ES definition, or the adjoint flux contribution.

Acknowledgments

The authors wish to express their gratitude to Dr. Kiefhaber and Dr. Vezzoni for their worthy advice and are obliged for to Dr. Maschek and Professor Ravetto for their priceless assistance.

Nomenclature

C	individual chromosome
FG	number of groups in the coarse ES
$f^{(k)}$	multiplication factor FF
$f^{(\Phi)}$	flux-based FF
$f^{(comb)}$	combined FF
f_I	fitness associated to individual I
g	generic group of the FL
G	generic group of the BL
MG	number of groups in the fine ES
φ	angular neutron flux
Φ	scalar neutron flux
R_I	ranking of individual I in its tournament

Conflicts of interest

All authors have no conflicts of interest to declare.

References

[1] H. Yamano, S. Fujita, Y. Tobita, K. Kamiyama, S. Kondo, K. Morita, E.A. Fischer, D.J. Brear, N. Shirakawa, X. Cao, M. Sugaya, M. Mizuno, S. Hosono, T. Kondo, W. Maschek, E. Kiefhaber, G. Buckel, A. Rineiski, M. Flad, T. Suzuki, P. Coste, S. Pigny, J. Louvet, T. Cadiou, SIMMER-III: A Computer Program for LMFR Core Disruptive Accident Analysis, JNC TN9400 2003-071, Japan Nuclear Cycle Development Institute, 2003.

[2] S. Kondo, H. Yamano, T. Suzuki, Y. Tobita, S. Fujita, X. Cao, K. Kamiyama, K. Morita, E.A. Fischer, D.J. Brear, N. Shirakawa, M. Mizuno, S. Hosono, T. Kondo, W. Maschek, E. Kiefhaber, G. Buckel, A. Rineiski, M. Flad, P. Coste, S. Pigny, J. Louvet, T. Cadiou, A Computer Program for LMFR Core Disruptive Accident Analysis, JNC TN9400 2001-002, Japan Nuclear Cycle Development Institute, 2000.

[3] M. Massone, F. Gabrielli, A. Rineiski, SIMMER extension for cross-section collapsing introduction, in: Proc. International Youth Nuclear Congress, Burgos, Spain, July 6–12, 2014, IYNC, 2014.

[4] M. Massone, F. Gabrielli, A. Rineiski, A genetic algorithm for multigroup energy structure search, Ann. Nucl. Energy 105 (2017) 369–387.

[5] M. Massone, F. Gabrielli, A. Rineiski, SIMMER extension for multigroup energy structure search using genetic algorithm, in: Proc. Int. Conf. M&C, Jeju, Korea, April 16–20, 2017, ANS, 2017.

[6] C. Yi, G. Sjoden, Energy group structure determination using particle swarm optimization, Ann. Nucl. Energy 56 (2013) 53–56.

[7] P. Mosca, A. Taofiki, P. Bellier, A. Prévost, Energy mesh optimization for multilevel calculation schemes, in: Proc. Int. Conf. M&C, Rio de Janeiro, Brazil, May 8–12, 2011, ANS, 2011.

[8] P. Mosca, C. Mounier, R. Sanchez, G. Arnaud, An adaptive energy mesh constructor for multigroup library generation for transport codes, Nucl. Sci. Eng. 167 (2011) 40–60.

[9] J.H. Holland, Outline for a logical theory of adaptive systems, J. ACM 9 (1962) 297–314.

[10] J.H. Holland, Adaptation in Natural and Artificial Systems, University Michigan Press, Ann Arbor, MI, USA, 1975.

[11] D.E. Goldberg, Genetic Algorithm in Search, Optimization and Machine Learning, Addison-Wesley Publishing Company, Boston, MA, USA, 1989.

[12] J.A. Anderson, An Introduction to Neural Networks, The MIT Press, Cambridge, MA, USA, 1995.

[13] T.H. Cormen, C.E. Leiserson, R.L. Rivest, C. Stein, Introduction to Algorithms, second ed., MIT Press and McGraw-Hill, Cambridge, MA, USA, 2001, pp. 214–217. ISBN 0-262-03293-7.

[14] D.E. Goldberg, K. Deb, A comparative analysis of selection schemes used in genetic algorithms, Found. Genet. Algor. 1 (1991) 69–93.

[15] A. Rineiski, V. Sinitsa, F. Gabrielli, W. Maschek, C4P cross-section libraries for safety analyses with SIMMER and related studies, in: Proc. Int. Conf. M&C, Rio de Janeiro, Brazil, May 8–12, 2011, ANS, 2011.

[16] E. Kiefhaber, Updating of an 11-groups Nuclear Cross Section Set for Transmutation Applications. FZKA-6480, Forschungszentrum Karlsruhe, 2000.

[17] S. Bortot, F. Alvarez y Velarde, E. Fridman, I.G. Cruzado, N.G. Herranz, D. López, K. Mikityuk, A.-L. Panadero, S. Pelloni, A. Ponomarev, P. Sciora, A. Seubert, H. Tsige-Tamirat, A. Vasile, European benchmark on the ASTRID-like low-void-effect core characterization: neutronic parameters and safety coefficients, in: Proc. ICAPP 2015, Nice, France, May 3–6, 2015, Société Française d'Énergie Nucléaire, 2015.

[18] InstitutsCluster II [Internet]. [Accessed 2017 Feb 6]. Available from: https://www.scc.kit.edu/dienste/ic2.php.

[19] B. Mcginley, F. Morgan, C. O'Riordan, Maintaining diversity through adaptive selection, crossover and mutation, in: Proc. GECCO 2008, Atlanta, Georgia, July 8–12, 2008, ACM, 2008.